J Solid State Electrochem (2000) 4: 383–389

ORIGINAL PAPER

Andrew J. Saterlay · Shelley J. Wilkins
Christiaan H. Goeting · John S. Foord
Richard G. Compton · Frank Marken

Sonoelectrochemistry at highly boron-doped diamond electrodes: silver oxide deposition and electrocatalysis in the presence of ultrasound

Received: 17 March 2000 / Accepted: 10 April 2000

Abstract The use of boron-doped diamond has a considerable impact in electrochemistry owing to the wide potential range accessible, low background currents, extreme hardness, and the ease of chemical modification of diamond surfaces. It is shown here that, although the electrodeposition of silver metal is known to yield very poorly adhering films with a poor electrical contact, a silver oxysalt deposit formed on anodically pre-treated diamond surfaces adheres strongly with good electrical contact. The deposit is stable even in the presence of ultrasound. Voltammetric and XPS studies reveal that the silver oxide deposit, in contrast to the silver metal deposit, is efficiently stripped from the diamond surface by applying a sufficiently negative potential. The silver oxysalt $Ag_7O_8NO_3$, deposited onto two types of boron-doped diamond electrodes, a 50 μm thick polycrystalline thin film deposited on a tungsten substrate and a polished free standing diamond plate, is shown to act as an electrocatalyst for oxygen evolution and for the oxidation of toluene. This development opens up the possibility of boron-doped diamond being applied as an inert and conducting substrate material for a wide range of oxidic materials, which can then be utilised as active electrocatalysts at high applied potentials.

Key words Electrocatalysis · Diamond · Ultrasound · Voltammetry · Silver oxide

Introduction

Boron-doped diamond electrode materials can be grown in a gas phase chemical vapour deposition (CVD) procedure and are available from industrial suppliers. The unusual properties of diamond such as extreme hardness and chemical inertness offer considerable potential for exploitation in a multitude of demanding electrochemical applications. The reversible deposition of lithium without intercalation [1], the selective analytical detection of serotonin and dopamine [2–6], waste water treatment [7], the reduction of nitrate [8], and the electrofluorination of difluorobenzene [9] are examples of interesting developments based on boron-doped diamond electrodes. Recent reviews give further details on the progress in this field [10–13].

Sonoelectrochemical methodology [14, 15] has been introduced to allow electrode processes to proceed under very fast mass transport conditions, with continuous electrode cleaning, and with further more subtle effects on nucleation and deposition processes. Applying power ultrasound has been shown to be very beneficial or even essential in several electroanalytical [16–18] and electrosynthetic [19–21] processes. However, owing to cavitation erosion and the considerable mechanical strain induced by the near-field high intensity ultrasonic waves, there are limitations for the type of electrode material employed and the power applied. With highly boron-doped diamond a novel type of electrode material is available with both a high mechanical hardness and a wide potential window ideal for applications of sonoelectrochemistry [22].

Both the boron-doping level [23] and the treatment of the diamond surface [24] have been shown to result in major changes in the rate and pathway of redox processes occurring at the diamond|solution interface. For a number of more complex electrode processes, very slow kinetics at bare diamond surfaces have been reported (for example, see [25]). On the other hand, some forms of deposit on boron-doped diamond allow very fast electron transfer with a good electrical contact to the electrode [26]. Under favourable conditions the modification of the diamond surface with a catalyst may allow a reaction pathway to be "selected" and the boron-doped diamond substrate may act as a versatile support with good electrical conductivity. A first report on the use of

A.J. Saterlay · S.J. Wilkins · C.H. Goeting · J.S. Foord
R.G. Compton · F. Marken (✉)
Physical and Theoretical Chemistry Laboratory,
Oxford University, Oxford OX1 3QZ, UK
e-mail: frank@physchem.ox.ac.uk

boron-doped diamond for an anodic electrocatalytic processs by Angus et al. [27] has appeared recently.

In the present study the oxidation of Ag^+ in aqueous media at boron-doped diamond electrodes and in the presence of power ultrasound is investigated. Under these conditions the formation of silver oxysalt deposits [28] on anodically pretreated boron-doped diamond electrodes is shown to result in a surface modification with strongly adhering and catalytically active characteristics. It is shown that in the presence of organic materials such as toluene, preferential oxidation of the organic substrate at the catalyst occurs. The combination of boron-doped diamond as highly conducting but inert substrate material with an electrocatalytically active metal oxide deposit is proposed as a new approach to efficient and selective electrocatalysis at high applied potentials.

Experimental

Reagents

Chemical reagents such as $K_4Fe(CN)_6$, $K_3Fe(CN)_6$, $AgNO_3$, KCl, KNO_3, and HNO_3 (all Aldrich) were obtained commercially in analytical or the highest available purity and used without further purification. Water was taken from an Elgastat filter system (Elga, High Wycombe, Bucks, UK) with a resistivity of not less than 18 Ohm cm. Argon (BOC, Pureshield) used as an inert atmosphere and hydrogen, methane, and diborane (BOC) used for CVD synthesis were used as supplied. Tungsten substrates (5 mm diameter rod, Goodfellows) were employed for the synthesis of boron-doped diamond films.

Instrumentation

The electrochemical cell [29] (volume 250 ml) employed for sonoelectrochemical measurements consisted of a glass cooling coil connected to a thermostatted bath, a platinum counter electrode, a saturated Calomel reference electrode (SCE, Radiometer Kopenhagen, REF 401), the diamond working electrode fitted into a Teflon holder and placed at the bottom of the cell facing the transducer horn tip, and an argon inlet. The ultrasonic processor, a Sonics & Materials VXC400 (20 kHz, 400 W) with 13 mm diameter titanium tip or a Hielscher UP200G system (24 kHz, 200 W) fitted with a 13 mm diameter glass horn (Dr. Hielscher, Stuttgart, Germany), were both electrically insulated from the electrochemical system and suitable for strongly acidic environments. The ultrasound intensity was determined calorimetrically [30, 31]. Electrochemical measurements were performed with a PGSTAT 20 AUTOLAB system (Eco Chemie, Netherlands) at a temperature of 25 ± 2 °C. The synthetic diamond films were characterised by scanning electron microscopy (SEM) with a JEOL JSM-5200 system, atomic force microscopy (AFM) with a Topometrix 2010 Discoverer system (Thermo Microscopes, Bicester, UK), and by Raman spectroscopy (Dilor Labram spectrometer with 20 mW He-Ne laser). The X-ray photoelectron spectra (XPS) were recorded at approximately 10^{-9} mbar with an ESCA300 using monochromatised Al Kα (1486.6 eV) X-ray radiation with 0.25 eV electron energy resolution.

Diamond electrodes

Two different types of boron-doped diamond electrodes were used. The first type consisted of a polycrystalline thin film deposit of diamond (50 μm thickness) grown on a 5 mm diameter tungsten support via a CVD procedure as described previously [32]. The Raman study of the film deposit indicates the presence of high quality diamond with a boron doping level of 10^{20}–10^{21} cm^{-3}. The surface of this polycrystalline diamond deposit is shown in Fig. 1a. The crystals size is typically 10–20 μm. In order to oxidise the surface of the diamond electrode, a potential cycling procedure employing 10 potential cycles over a potential range from 0 to 3 V vs. SCE in 0.2 M phosphate buffer at pH = 2 was employed [32].

Further, a free-standing plate of boron-doped diamond (De Beers Industrial Diamond Division, Ascot, UK) of 5 × 5 × 0.6 mm dimensions [24] was employed, mounted in a Teflon housing using Araldite (Ciba Polymers, CY219), with an electrical connection to the rear side via a brass rod, attached using silver epoxy resin (RS). Raman spectra of this diamond material also are consistent with high quality diamond with a boron-doping level of 10^{19}–10^{20} cm^{-3}. The surface of this diamond electrode, which was obtained in a polished state (see Fig. 1b), is smooth to a nanometer scale with only small imperfections between crystal boundaries.

Results and discussion

Sonovoltammetric oxidation of $Fe(CN)_6^{4-}$ at a boron-doped diamond thin film electrode

Cyclic voltammetric experiments with boron-doped diamond electrodes employing the $Fe(CN)_6^{3-/4-}$ redox couple (Eq. 1) in aqueous KCl provided a suitable redox system for the characterisation of the diamond electrode surface properties [33] and the mass transport under diffusion limiting conditions:

$$Fe(CN)_6^{3-} + e^- \rightleftharpoons Fe(CN)_6^{4-} \quad (1)$$

In Fig. 2 a cyclic voltammogram together with a sonovoltammogram are shown. The 5 mm diameter polycrystalline boron-doped diamond electrode has been activated prior to the experiment by anodising in 0.2 M phosphate buffer at pH 2 by cycling the potential up to + 3.0 V vs. SCE in phosphate buffer (see Experimental). Well-defined cyclic voltammetric responses for the $Fe(CN)_6^{3-/4-}$ redox system can be observed.

In the presence of ultrasound the current increases considerably (Fig. 2b). The high limiting current, I_{lim} = 0.53 mA, is predominantly due to the flow of liquid close to the electrode surface induced by the high intensity ultrasound on macro and micro scales [34]. The limiting current for the oxidation of 1 mM $Fe(CN)_6^{4-}$ in aqueous 0.1 M KCl induced by the 24 kHz insonation with the glass horn may be used to estimate the diffusion layer thickness, δ, a parameter describing the rate of mass transport (Eq. 2):

$$I_{lim} = \frac{n F D A c}{\delta} \quad (2)$$

In this equation the limiting current, I_{lim}, is determined by n, the number of electrons transferred per molecule in the redox process, F, the Faraday constant, D, the diffusion coefficient, A, the area of the electrode, c, the concentration, and the diffusion layer thickness, δ. For the conditions used in Fig. 2 and a diffusion coefficient [35] of $D(Fe(CN)_6^{4-}) = 0.65 \times 10^{-9}$ m^2 s^{-1}, a typical

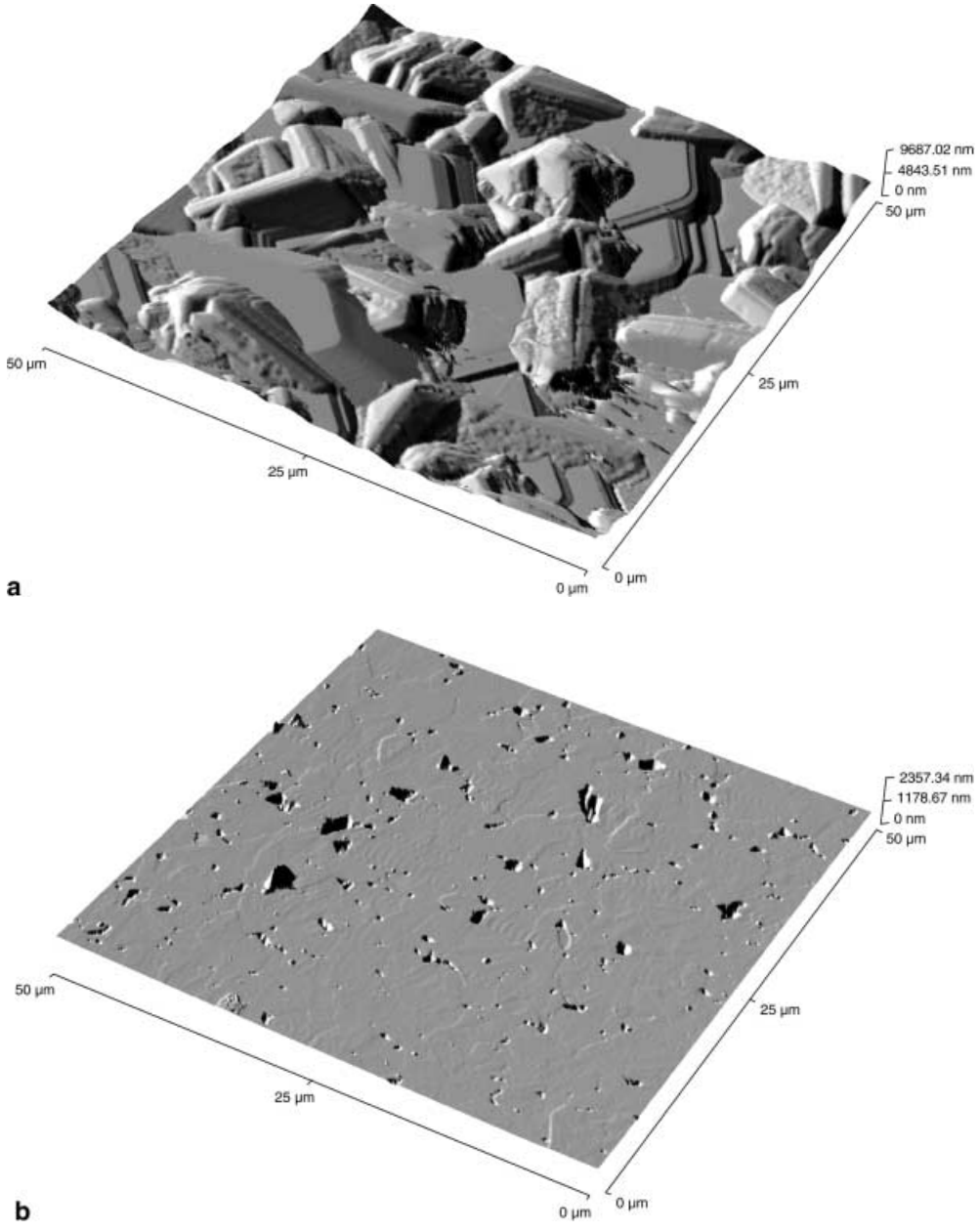

Fig. 1a,b AFM images of boron-doped diamond electrodes: **a** surface of an "as grown" diamond film on a tungsten substrate and **b** a polished boron-doped diamond surface (De Beers)

diffusion layer thickness of 9 µm can be determined. By varying the distance between horn emitter and working electrode, diffusion layer thicknesses of less than 1 µm are accessible [34]. More detailed models for the mass transport induced by ultrasound in aqueous media have been proposed [36] but are not essential in the context of the present study.

Sonovoltammetric oxidation of Ag^+ at boron-doped diamond electrodes

The voltammetric reduction and oxidation of Ag^+ dissolved in aqueous solution at a boron-doped diamond electrode in the absence of ultrasound has been studied by several authors [37, 38]. Recent work by Vinokur et al. [28] gives a detailed account of the mechanism of the electrochemical deposition of both silver metal and silver oxysalts onto boron-doped diamond surfaces. The oxidation of Ag^+ to Ag^{2+} is a commercially important process for the detoxification of wastes [39, 40] and more specifically the degradation of toxic organic compounds [41]. This process has to be conducted in the presence of high concentrations of nitric acid to solubilise the Ag^{2+} cation.

Voltammetric responses for the reduction and oxidation of 1 mM Ag^+ at a 5 mm diameter polycrystalline boron-doped diamond electrode in the presence of an acidic supporting electrolyte, HNO_3, are shown in Fig. 3. The onset of the reduction process (Eq. 3) can be seen to lead to the slow increase of the cathodic current until a limiting current, $I_{lim} = 0.48$ mA, is reached:

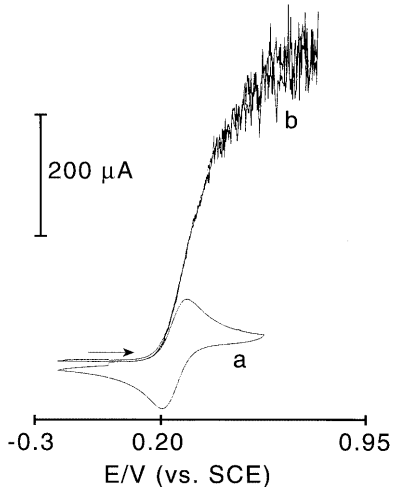

Fig. 2 a Cyclic voltammogram for the oxidation of 1 mM $Fe(CN)_6^{4-}$ obtained in 0.1 M KCl solution at a 5 mm diameter boron-doped diamond film electrode with a scan rate of 0.1 V s^{-1}. **b** Cyclic sonovoltammogram obtained under the same conditions (30 W cm^{-2}, 24 kHz ultrasound, 10 mm electrode to horn distance)

$$Ag^+(aq) + e^- \rightleftharpoons Ag(solid) \quad (3)$$

This diffusion-controlled limiting current is consistent with a diffusion layer thickness of $\delta = 23$ μm based on a diffusion coefficient of $D_{Ag^+} = 1.5 \times 10^{-9}$ m^2 s^{-1} [42] (Eq. 2). The diffusion-controlled limiting current associated with the deposition of silver metal remains constant until at a potential of 0.25 V vs. SCE, when anodic stripping of the metal deposit commences.

The current fluctuation superimposed on the sonovoltammetric limiting current is in agreement with mass transport control [14, 15]. It is interesting to note the effect of increasing the supporting electrolyte concentration. On the polycrystalline thin film diamond electrode, both the reduction and the "stripping" process become substantially less well-defined in the presence of a higher concentration of supporting electrolyte (Fig. 3). The metal stripping process has been shown to be incomplete, with silver metal deposit left behind on the surface of the diamond electrode after the potential has been scanned positive of the stripping process [28]. An SEM and XPS study on the state of the polycrystalline boron-doped diamond electrode surface immersed in 1 mM Ag^+ in 1 M HNO_3 after cycling the potential to −0.25 V vs. SCE and back to 0.75 V vs. SCE with a scan rate of 0.1 V s^{-1} revealed that, even after stripping the silver metal deposit, the electrode surface remained partially covered with silver metal. SEM images in backscatter mode indicate approximately 0.4% surface area covered with silver.

The oxidation of aqueous Ag^+ in the presence of NO_3^- is known to yield a deposit of a silver oxysalt [43] with a composition $Ag_7O_8NO_3$ (Eq. 4). Only in the presence of high concentrations of acid is the Ag^{2+} cation sufficiently soluble to be formed directly.

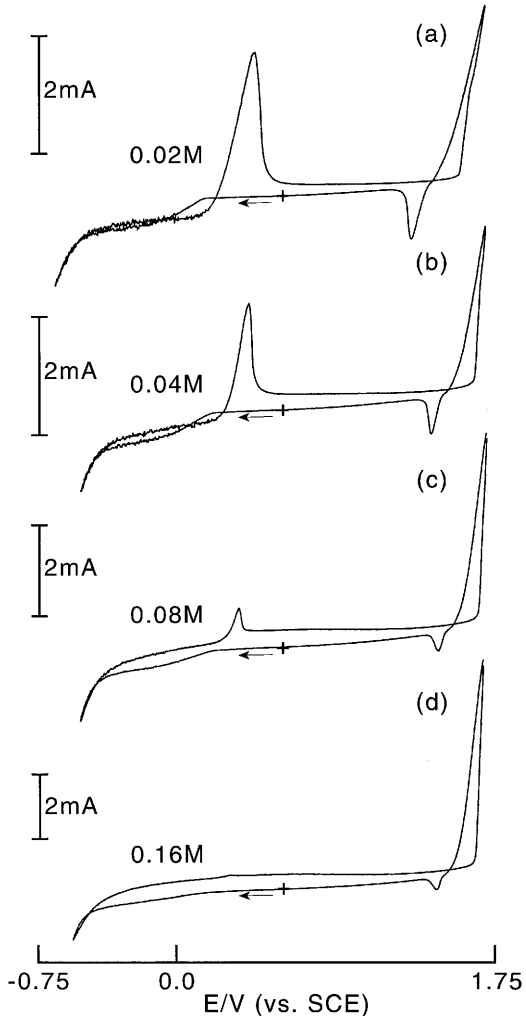

Fig. 3 Cyclic sonovoltammograms for the reduction and oxidation of 1 mM Ag^+ obtained in HNO_3 solution (concentration **a** 0.02 M, **b** 0.04 M, **c** 0.08 M, **d** 0.16 M) at a 5 mm diameter boron-doped diamond film electrode with a scan rate of 0.1 V s^{-1}, 30 W cm^{-2}, 24 kHz ultrasound and 12 mm electrode to horn distance

$$7Ag^+(aq) + 8H_2O + NO_3^-(aq) \rightleftharpoons Ag_7O_8NO_3\ (solid) + 10e^- + 16H^+(aq) \quad (4)$$

In Fig. 3 it can be seen that the oxidation process is followed by a characteristic stripping peak upon reversal of the scan direction. Both the onset of the deposition process and the potential for the stripping process are affected by the concentration of nitric acid. In Fig. 4a voltammograms obtained for the oxidation of 1 mM Ag^+ in aqueous HNO_3 at a polished boron-doped diamond electrode are shown. At this type of diamond surface, very similar voltammetric characteristics are observed. The onset of silver oxysalt deposition as well as the stripping response shift to more positive potentials as the concentration of protons is increased. The onset potentials of the stripping peaks exhibit a characteristic shift of approximately 95 mV per unit pH change, in agreement with the process described by Eq. 4. In

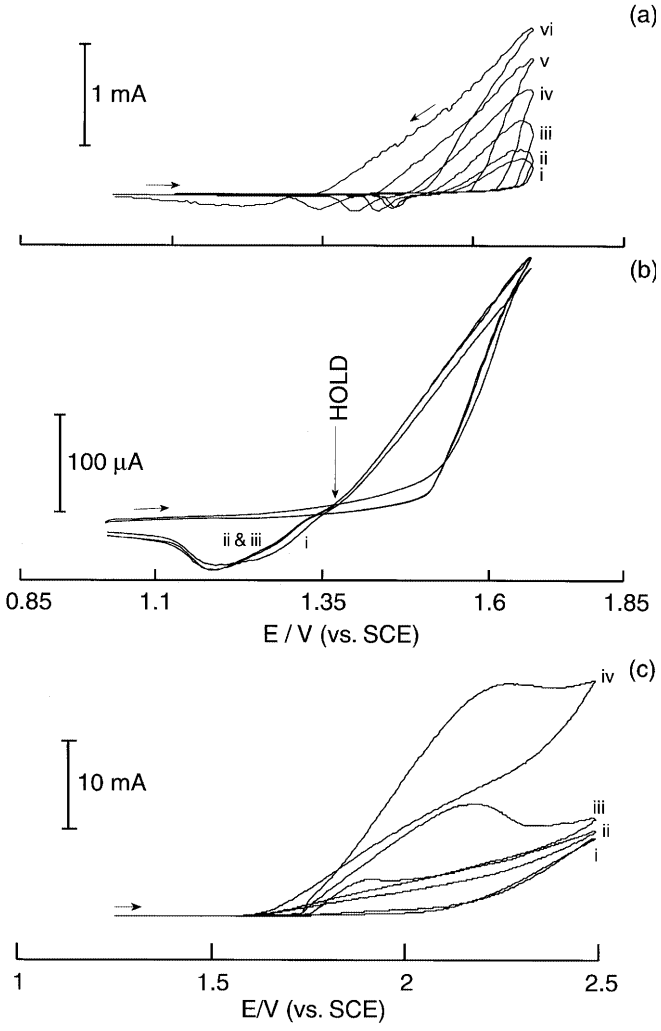

Fig. 4 a Cyclic voltammograms for the oxidation of 1 mM Ag^+ obtained in 0.1 M HNO_3 at pH *i* 1.09, *ii* 1.14, *iii* 1.31, *iv* 1.62, *v* 2.15, and *vi* 3.14 (pH adjusted by addition of 10 M NaOH). **b** Cyclic voltammograms for the oxidation of 1 mM Ag^+ obtained in 1 mM HNO_3 *i* under continuous ultrasonic irradiation (38 W cm^{-2}, 10 mm horn to electrode separation), *ii* ultrasound during oxidation, potential held at 1.375 V vs. SCE for 120 s (silent), silent reduction, and *iii* as in *i* except held at 1.375 V vs. SCE for 60 s during negative sweep. **c** Cyclic voltammograms for the oxidation of Ag^+ *i* 12 μM, *ii* 258 μM, *iii* 510 μM, and *iv* 1.96 mM in 0.1 M HNO_3

Fig. 4b the effect of ultrasound on the silver oxysalt deposit formation in a solution containing 1 mM Ag^+ and 1 mM HNO_3 is demonstrated. The response (i) has been obtained by cycling the potential with 0.1 V s^{-1} in the presence of 38 W cm^{-2} ultrasound. Switching the ultrasound off at a potential of 1.375 V vs. SCE and holding the potential for 120 s has only a minor effect (response ii). Holding the potential scan at a potential at which no further deposition occurs, $E = +1.375$ V vs. SCE, in the presence of ultrasound can be seen (response iii) to lead to a virtually identical voltammetric trace. Therefore both further deposition at a potential of +1.375 V vs. SCE and the removal of the silver oxysalt deposit by ultrasound-induced interfacial cavitation can be ruled out. The deposit appears to remain rigidly attached. Aside from the electrosynthetic possibilities discussed here, the silver oxysalt deposition and stripping procedure offers scope for development into a quantitative analytical method (Saterlay AJ, Marken F, Foord JS, Compton RG, submitted).

The cathodic stripping process in which the silver oxysalt is reduced back to Ag^+(aq) is relatively fast, in contrast to the stripping of metal deposits (vide supra). An SEM and XPS study of a polycrystalline boron-doped diamond electrode on a tungsten substrate immersed in 1 mM Ag^+ (1 M HNO_3) after cycling the potential from 0.5 V vs. SCE to 1.75 V vs. SCE and back with a scan rate of 0.1 V s^{-1} revealed that, in this case, no silver deposit remains on the electrode surface at 0.5 V vs. SCE. That is, the electrical contact between electrode and deposit is good and the stripping process essentially complete. The considerable mismatch between anodic and cathodic current can be explained via a catalytic process in which water is oxidised to oxygen. In Fig. 3 it can be seen that, at the potential at which the silver oxysalt deposition commences, there is an immediate increase in anodic current. This current is considerably higher than that expected for the mass transport controlled deposition process.

The effect of the concentration of Ag^+ on the voltammetric response for the formation and stripping of $Ag_7O_8NO_3$ in the absence of ultrasound is shown in Fig. 4c. The catalytic current associated with the water oxidation develops even at a very low concentration of 12 μM Ag^+ in 0.1 M aqueous HNO_3 (response i). However, the rapid increase in current is much more pronounced at higher concentration. The peak-shaped feature is probably associated with the depletion of silver from the solution during the deposition process and/or the formation of gas bubbles on the electrode surface in the absence of ultrasound.

By increasing the concentration of acid to 6 M HNO_3 the formation of the silver oxysalt deposit ceases (not shown); however, the anticipated formation of soluble Ag^{2+} at the boron-doped diamond electrode surface still cannot be detected even up to potentials of 2.5 V vs. SCE. It appears likely that the heterogeneous electron transfer for the $Ag^{2+/+}$ redox couple is associated with slow kinetics at diamond electrodes in the presence of a high concentration of HNO_3.

At lower concentration of HNO_3, silver oxysalt is formed which is acting as catalyst for the formation of oxygen. After the onset of silver oxysalt deposition the dramatic rise in anodic current (Fig. 3) suggests a high catalytic activity and a good electrical contact between oxide deposit and diamond surface. The finding may be interpreted in terms of highly boron-doped diamond being a very good conductor for electrical charges and a very good substrate for carrying active catalyst materials. Recent work on the anodic deposition of other types of metal oxides, such as PbO_2 and MnO_2, on boron-doped diamond surfaces [44, 45] demonstrates the general applicability of the method.

Sonovoltammetric oxidation of toluene
at modified boron-doped diamond electrodes

The voltammetric characteristics of the silver oxysalt deposit suggest that a high catalytic activity of the deposit is responsible for the high anodic current observed at a potential of approximately 1.6 V vs. SCE (Fig. 3). The presence of organic materials in the aqueous solution phase can be shown to have a considerable effect on the voltammetric response for the silver oxysalt formation and the catalytic current. Here, toluene is used as a model system in order to explore the possibility of diamond-based electrocatalysis. The oxidation of toluene in the presence of a homogeneous silver catalyst has been studied [46–48] and benzaldehyde has been identified as the main product. In Fig. 5a it can be seen that the presence of toluene, employing a saturated solution with 0.4 volume% toluene emulsified in 0.5 M HNO_3, causes the onset of the anodic current response to shift to more positive potentials. That is, the deposition of the silver oxysalt requires a higher overpotential in the presence of toluene. However, once the catalytically active deposit is formed the current increases considerably compared to the current observed in the absence of toluene. Also the current response during the reverse potential scan is increased. That is, the silver oxysalt deposit is preferentially oxidising the organic material even in the presence of a huge excess of water. In the presence of ultrasound, very similar characteristics can be observed (Fig. 5b). The formation of the silver oxysalt deposit occurs at a more positive potential in the presence of ultrasound and the current associated with the oxidation of toluene appears to be increased. However, the mass transport enhancement, which is known to strongly affect kinetically fast processes, is rather small and the process may therefore be considered to be controlled by the kinetics of the heterogeneous process. Mechanistic details, such as the ratio of oxygen evolution and toluene oxidation in the presence of ultrasound and the distribution of products formed in this oxidation process, are under further investigation.

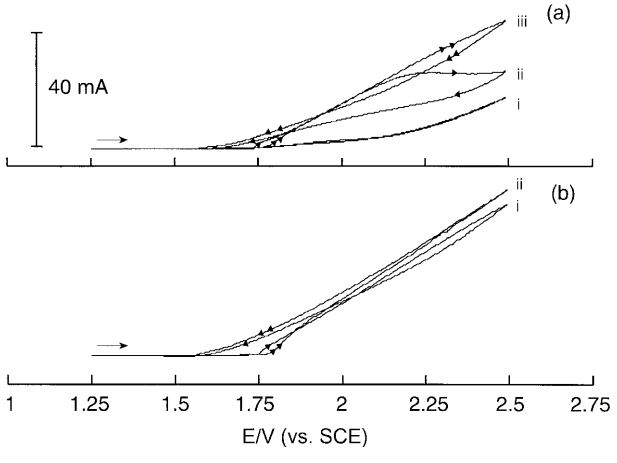

Fig. 5 a Cyclic voltammograms obtained for *i* 0.5 M HNO_3, *ii* in the presence of 3.64 mM Ag^+, and *iii* in the presence of 3.64 mM Ag^+ and 0.4 volume% toluene emulsion. **b** Cyclic voltammograms obtained for the oxidation of 1.96 mM Ag^+ in a 0.4 volume% toluene/0.5 M HNO_3 emulsion: *i* under silent conditions, *ii* under ultrasound irradiation (38 W cm^{-2}, 10 mm horn to electrode separation)

Conclusions

Boron-doped diamond is a versatile electrode material not only in bare or surface-modified form, but it may also act as substrate material in electrocatalysis. In particular, metal oxide deposits appear to form on anodised diamond with good adhesion and good electrical conductivity. The wide potential window accessible with boron-doped diamond may therefore allow thin layers of metal oxide deposits to be employed in electrocatalytic processes even in cases in which the oxide itself is not sufficiently electrically conducting. Further, the use of power ultrasound to enhance the rate of the heterogeneous electrocatalytic process is possible and may lead to higher efficiencies, especially in the case of reactions with low substrate concentrations.

Acknowledgements F.M. thanks the Royal Society for a University Research Fellowship and New College, Oxford, for the award of a stipendiary Lectureship. S.J.W. thanks Glaxo Wellcome and BBSRC for a CASE award. G. Scarsbrook, R.S. Sussmann, and A.J. Whitehead (De Beers Industrial Diamond Division, UK) are gratefully acknowledged for generous support of the diamond project. A.J.S. thanks Alcan and the EPSRC for a CASE studentship and the EPSRC for financial support.

References

1. Li LF, Totir D, Miller B, Chottiner G, Argoitia A, Angus JC, Scherson D (1997) J Am Chem Soc 119: 7875
2. Strojek JW, Granger MC, Swain GM, Dallas T, Holtz MW (1996) Anal Chem 68: 2031
3. Popa E, Notsu H, Miwa T, Trk DA, Fujishima A (1999) Electrochem Sol State Lett 2: 49
4. Silva SM, Alves CR, Machado SAS, Mazo LH, Avaca LA (1996) Electroanalysis 8: 1055
5. Sarada BV, Rao TN, Tryk DA, Fujishima A (1999) Chem Lett 1213
6. Fujishima A, Rao TN, Popa E, Sarada BV, Yagi I, Tryk DA (1999) J Electroanal Chem 473: 179
7. Fryda M, Herrmann D, Schafer L, Klages CP, Perret A, Haenni W, Comninellis C, Gandini D (1999) New Diamond Frontier Carbon Technol 9: 229
8. Bouamrane P, Tadjeddine A, Butler JE, Tenne R, LevyClement C (1996) J Electroanal Chem 405: 95
9. Okino F, Shibata H, Kawasaki S, Touhara H, Momota K, Nishitani-Gamo M, Sakaguchi L, Ando T (1999) Electrochem Solid State Lett 2: 382
10. Swain GM, Anderson AB, Angus JC (1998) MRS Bull 56
11. Xu J, Granger MC, Chen Q, Strojek JW, Lister TE, Swain GM (1997) Anal Chem 69: 591A
12. Pleskov YuV (1999) Russ Chem Rev 68: 381
13. Goeting CH, Marken F, GutierrezSosa A, Compton RG, Foord JS (1999) New Diamond Frontier Carbon Technol 9: 207
14. Walton DJ, Phull SS (1996) Adv Sonochem 4: 205

15. Compton RG, Eklund JC, Marken F (1997) Electroanalysis 9: 509
16. Blythe AN, Akkermans RP, Compton RG (2000) Electroanalysis 12: 16
17. Davis J, Compton RG (2000) Anal Chim Acta 404: 241
18. Ball JC, Compton RG (1999) Electrochemistry 67: 912
19. Marken F, Compton RG, Buston JEH, Moloney MG (1998) Electroanalysis 10: 1188
20. Atobe M, Tonoi T, Nonaka T (1999) Electrochem Commun 1: 593
21. Atobe M, Yamada N, Nonaka T (1999) Electrochem Commun 1: 532
22. Goeting CH, Foord JS, Marken F, Compton RG (1999) Diamond Relat Mater 8: 824
23. LevyClement C, Zenia F, Ndao NA, Deneuville A (1999) New Diamond Frontier Carbon Technol 9: 189
24. Compton RG, Marken F, Goeting CH, McKeown RAJ, Foord JS, Scarsbrook G, Sussmann RS, Whitehead AJ (1998) J Chem Soc Chem Commun 1961
25. Alehashem S, Chambers F, Strojek JW, Swain GM (1995) Anal Chem 67: 2812
26. Marken F, Compton RG, Goeting CH, Foord JS, Bull SD, Davies SG (2000) J Solid State Electrochem 4: (in press)
27. Angus JC, Martin HB, Landau U, Evstefeeva YE, Miller B, Vinokur N (1999) New Diamond Frontier Carbon Technol 9: 175
28. Vinokur N, Miller B, Avyigal Y, Kalish R (1999) J Electrochem Soc 146: 125
29. Compton RG, Eklund JC, Marken F, Rebbitt TO, Akkermans RP, Waller DN (1997) Electrochim Acta 42: 2919
30. Margulis MA, Mal'tsev AN (1969) Russ J Phys Chem 43: 592
31. Mason TJ, Lorimer JP, Bates DM (1992) Ultrasonics 30: 40
32. Goeting CH, Marken F, Gutierrez-Sosa A, Compton RG, Foord JS (2000) Diamond Relat Mater 9: (in press)
33. Yagi I, Notsu H, Kondo T, Tryk DA, Fujishima A (1999) J Electroanal Chem 473: 173
34. Marken F, Akkermans RP, Compton RG (1996) J Electroanal Chem 415: 55
35. Adams RN (1969) Electrochemistry at solid electrodes, Marcel Dekker, New York, p 219
36. Hill HAO, Nakagawa Y, Marken F, Compton RG (1996) J Phys Chem 100: 17395
37. Ramesham R (1999) J Mater Sci 34: 1439
38. Goeting CH, Marken F, Salter C, Compton RG, Foord JS (1999) J Chem Soc Chem Commun 1697
39. Fleischmann M, Pletcher D, Rafinski A (1971) J Appl Electrochem 1: 1
40. Farmer JC, Wang FT, Hawleyfedder RA, Lewis PR, Summers LJ, Foiles L (1992) J Electrochem Soc 139: 654
41. Hickman RG, Farmer JC, Wang FT (1993) ACS Symp Ser 518: 430
42. Mills R, Lobo VMM (1989) Self-diffusion in electrolyte solutions. Elsevier, Amsterdam
43. Breyfogle BE, Hung CJ, Shumsky MG, Switzer JA (1996) J Electrochem Soc 143: 2741
44. Saterlay AJ, AgraGutierrez C, Taylor MP, Marken F, Compton RG (1999) Electroanalysis 11: 1083
45. Saterlay AJ, Foord JS, Compton RG (1999) Analyst 124: 1791
46. Otsuka K, Ishizuka K, Yamanaka I, Hatano M (1991) J Electrochem Soc 138: 31762
47. Jow JJ, Chou TC (1988) J Appl Electrochem 18: 298
48. Lee AC, Chou TC (1995) Chem Eng J Biochem Eng J 56: 1